Journal of Microencapsulation
Micro and Nano Carriers

ISSN: (Print) (Online) Journal homepage: https://www.tandfonline.com/loi/imnc20

Dual drug loaded polypeptide delivery systems for cancer therapy

Natalia Zashikhina, Erik Gandalipov, Apollinariia Dzhuzha, Viktor Korzhikov-Vlakh & Evgenia Korzhikova-Vlakh

To cite this article: Natalia Zashikhina, Erik Gandalipov, Apollinariia Dzhuzha, Viktor Korzhikov-Vlakh & Evgenia Korzhikova-Vlakh (12 Oct 2023): Dual drug loaded polypeptide delivery systems for cancer therapy, Journal of Microencapsulation, DOI: 10.1080/02652048.2023.2270064

To link to this article: https://doi.org/10.1080/02652048.2023.2270064

JOURNAL OF MICROENCAPSULATION
https://doi.org/10.1080/02652048.2023.2270064

Taylor & Francis
Taylor & Francis Group

RESEARCH ARTICLE

Dual drug loaded polypeptide delivery systems for cancer therapy

Natalia Zashikhina[a], Erik Gandalipov[b], Apollinariia Dzhuzha[c], Viktor Korzhikov-Vlakh[a,c] and Evgenia Korzhikova-Vlakh[a,c]

[a]Institute of Macromolecular Compounds, Russian Academy of Sciences, St. Petersburg, Russia; [b]International Institute of Solution Chemistry and Advanced Materials Technologies, ITMO University, St. Petersburg, Russia; [c]Institute of Chemistry, Saint-Petersburg State University, St. Petersburg, Russia

ABSTRACT

The present study was aimed to prepare and examine *in vitro* novel dual-drug loaded delivery systems. Biodegradable nanoparticles based on poly(L-glutamic acid-*co*-D-phenylalanine) were used as nanocarriers for encapsulation of two drugs from the paclitaxel, irinotecan, and doxorubicin series. The developed delivery systems were characterised with hydrodynamic diameters less than 300 nm (PDI $<$ 0.3). High encapsulation efficiencies ($\geq$75%) were achieved for all single- and dual-drug formulations. The release studies showed faster release at acidic pH, with the release rate decreasing over time. The release patterns of the co-encapsulated forms of substances differed from those of the separately encapsulated drugs, suggesting differences in drug-polymer interactions. The joint action of encapsulated drugs was analysed using the colon cancer cells, both for the dual-drug delivery sytems and a mixture of single-drug formulations. The encapsulated forms of the drug combinations demonstrated comparable efficacy to the free forms, with the encapsulation enhancing solubility of the hydrophobic drug paclitaxel.

ARTICLE HISTORY
Received 18 April 2023
Accepted 9 October 2023

KEYWORDS
Polypeptides; polymeric particles; antitumor drugs; irinotecan; doxorubicin; paclitaxel; co-encapsulation; combination of drugs; dual drug delivery systems

1. Introduction

Cancer is still an undefeated disease. Great efforts of scientists from various fields are directed to this area, however, only limited progress is observed. The majority of drugs under development do not demonstrate the expected therapeutic efficiency. Furthermore, most of the failed cases in cancer therapy are due to cancer chemoresistance (Hu et al., 2010). Drug resistance can include different mechanisms such as alteration in signalling pathways and drug targets, the presence of molecular efflux pumps, increased DNA repair processes and cell death inhibition (Housman et al. 2014, Mansoori et al. 2017, Ghosh et al. 2019, Zhou et al. 2020).

Various strategies are used to overcome this drawback, and the most promising are the application of delivery systems (Ambrosio Téllez et al. 2022, Ambrosio et al. 2023) and synergistic combinations of different therapeutics (Gadde 2015, Miao et al. 2017, Pushpalatha et al. 2017). In current literature combinations of such anti-tumour drugs as paclitaxel (Katragadda et al. 2011), doxorubicin (Liu et al. 2019), cisplatin (Mehnath et al. 2018), daunorubicin (Tardi et al. 2009), floxuridine and irinotecan (Tardi et al. 2007) which non-specifically eliminate all rapidly dividing cells, are discussed. However, combining drugs can either reduce the required dose of chemotherapy while maintaining high efficacy or cause side effects. Overall, this approach is still far from being perfect and requires considerable optimisation (Hu et al. 2010). In turn, delivery systems can increase the effectiveness of the drug due to the targeted transport to affected cells by overcoming various biological barriers to delivery, the preservation of the activity of the drug molecule, the reduction of side effects, changes in biodistribution and increased efficacy compared to the conventional drugs (El-Say and El-Sawy 2017, Patra et al. 2018, Yao et al. 2020, Mitchell et al. 2021). Thus, combining these two strategies into one system is supposed to be another step in the development of antitumor therapy. The co-delivery approach can be based on joint administration of different single drug-containing nanoparticles as well as multidrug-loaded particles (Greco and Vicent 2009, Hu et al. 2010). In the latter case, a uniformity of carriers defines the features of systems such as a co-release.

Drug encapsulation can be achieved through physical encapsulation, chemical conjugation and

CONTACT Evgenia Korzhikova-Vlakh vlakh@hq.macro.ru, vlakh@mail.ru Institute of Macromolecular Compounds, Russian Academy of Sciences, Bolshoy pr. 31, St. Petersburg 199004, Russia

electrostatic interactions, depending on the chemical nature of the drug molecule (Iyer et al. 2013, Xu et al. 2015, Hu et al. 2016). Currently, this co-loading approach is applied to systems such as liposomes (Morton et al., 2014, Liu et al. 2019, Lin et al. 2019), poly(lactic-co-glycolic acid)-based (PLGA) (Kolishetti et al. 2010, Tian et al. 2017, Do et al. 2018) and polycaprolactone-based (PCL) particles (Milane et al. 2011), polysaccharide (Xiao et al. 2015a, 2015b) and polypeptide-based nanoparticles (Zheng et al. 2013, Zhang et al. 2016), PEG conjugate (Zhang et al. 2016), and polyphosphazene-based multilayer nanoparticles (Mehnath et al. 2018). Many liposomal and polymeric formulations are being investigated in the preclinical/clinical studies. These co-encapsulated systems have demonstrated a synergistic effect and increased efficiency of the delivery system, resulting in significant therapeutic outcomes both *in vitro* and *in vivo*. For instance, a liposomal system combining PTX and DOX was tested in the pre-clinical trials (Roque et al. 2021). The combined system was found to be effective for the treatment of breast cancer while exhibiting reduced toxicity compared to the mixture of free drugs. Recently, Pitchika et al. reported the development of PTX and lapatinib (LPB) dual loaded chitosan-coated PLGA nanoparticles to overcome multi-drug resistance in breast cancer therapy (Pitchika and Sahoo 2022). The co-delivery of PTX and LPB demonstrated the most effective tumour growth reduction in the BT-474/TR human breast tumour xenograft compared to controls. Additionally, PTX and curcumin (Lin et al. 2023), as well as DOX and vemurafenib (D'Angelo et al. 2022) combined delivery systems based on PEG-PLGA and PEG-poly(ε-caprolactone), respectively, have been recently developed to overcome the cancer chemoresistance.

Among various polymers, polypeptides offer several advantages for drug delivery (Gao et al. 2020, Georgilis et al. 2020). They are biocompatible and biodegradable (Shah et al., 2012) and can be tailored by adjusting their size, surface charge, and functionalization to optimise drug delivery performance (Zashikhina et al. 2017, Jacobs et al. 2019, Yang et al. 2022). They can exhibit stimuli-responsive behaviour, triggering drug release in response to specific environmental cues (He et al. 2012, Wang et al. 2021). Earlier, it was shown that self-assembled polypeptide nanoparticles (NPs) can be used for the encapsulation of anti-tumour drugs (Zashikhina et al. 2017, Zashikhina et al. 2022). In particular, poly(L-glutamic acid-*co*-D-phenylalanine) (P(Glu-*co*-DPhe)) is a biodegradable polypeptide which, being amphiphilic, demonstrates the ability to self-assemble in aqueous media into spherical nanoparticles (Figure 1). The formed NPs are stabilised by hydrophobic interactions between Phe units inside the nanoparticles and possess carboxyl groups on their surface. Being negatively charged, they exhibit stability against aggregation, low cytotoxicity, and a low rate of uptake by macrophages (Iudin et al. 2020).

In this study, we propose the use P(Glu-*co*-DPhe) as delivery system for two different anti-tumour drugs representing combinations of paclitaxel, irinotecan and doxorubicin (Figure 2). These substances were selected mostly as model chemotherapeutics based on their physicochemical properties allowing us to investigate the main features of such systems, such as co-encapsulation, release patterns and cytotoxic effect. It is worth noting that the used combinations have potential applications in the treatment of various cancer types, such as ovarian cancer, lung cancer, colorectal cancer, breast cancer, and others. Encapsulation of hydrophobic paclitaxel was accomplished through hydrophobic interactions with the core of nanoparticles, while the loading of irinotecan and doxorubicin was achieved due to ionic interactions with the carboxylic groups of P(Glu-*co*-DPhe). The release rate and the mechanisms of drug release were studied and compared for the single and dual drug delivery systems. To study the drug dissolution mechanisms the release profiles were analysed with a number of mathematical models. Furthermore, the biological activity of free, encapsulated and co-encapsulated forms with the use of colon cancer cells (HCT-116 cell line) was investigated and a comparative analysis was carried out.

2. Materials and methods

2.1. Materials

Triphosgene (98%), α-pinene (98%), hexylamine (HexNH2, 99%), L-glutamic acid γ-benzyl ester (≥99%), D-phenylalanine (D-Phe, ≥98%), trifluoroacetic acid (TFA, 99%), trifluoromethanesulfonic acid (TFMSA, 98%) were purchased from Sigma-Aldrich GmbH (Germany) and used as received. Doxorubicin hydrochloride (≥99%), paclitaxel (≥99.5%) and irinotecan hydrochloride trihydrate (>98.5%) were purchased from Bld Pharmatech (China). Solvents: N,N-dimethylformamide (DMF), ethyl acetate, n-hexane, were product of Vecton Ltd. (Russia) and distilled before use.

Dialysis membrane Zellu Trans Dialysis Tubes T2 with molecular weight cut-off (MWCO) 3500 were purchased from Scienova GmbH (Germany) and dialysis

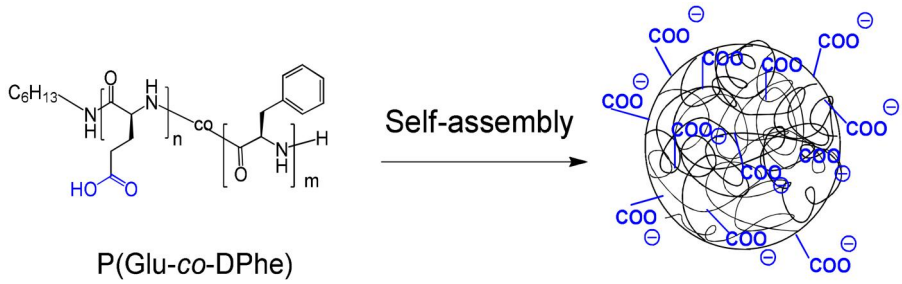

Figure 1. Scheme for preparation of self-assembled P(Glu-co-DPhe)-based nanoparticles (gradient phase inversion method from DMF to water (dialysis)).

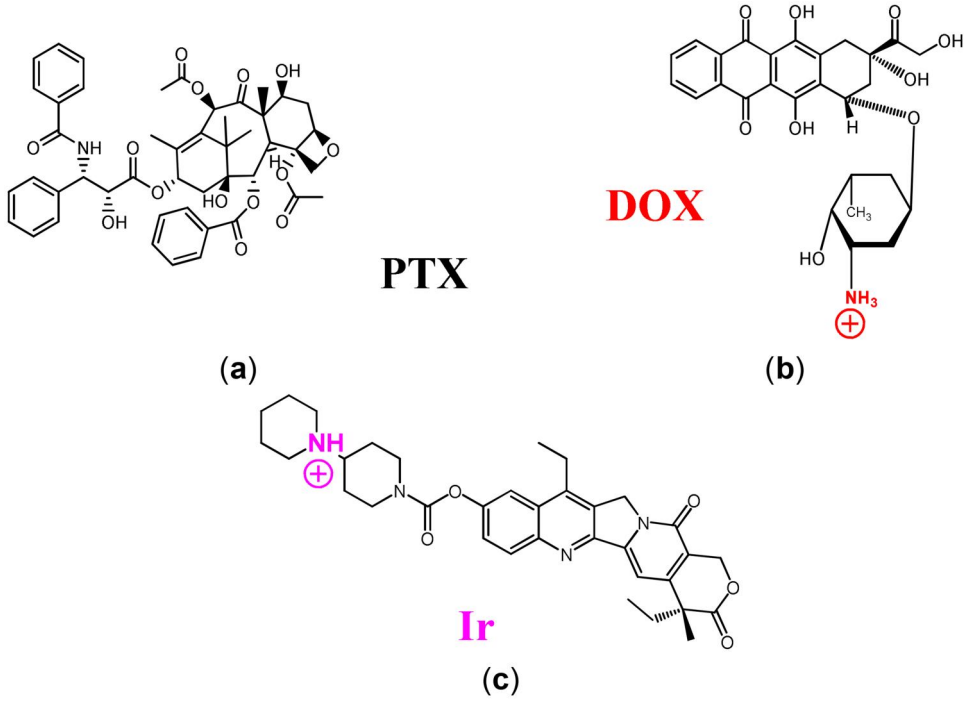

Figure 2. Chemical structures of the anti-tumour substances used in the work: (a) paclitaxel (PTX), (b) doxorubicin (DOX), (c) irinotecan (Ir).

tubes GeBAflex Mini and Maxi (MWCO 3500) were the product of Scienova GmbH (Germany).

Human colorectal cancer cells (HCT-116 cell line) were purchased from ATCC (USA). HCT-116 cells were cultivated in Dulbecco's Modified Eagle's Medium (DMEM, Biolot, Russia) supplemented with 10% (v/v) fetal bovine serum (FBS) (Biowest, France), and 50 μg/mL gentamicin (Biolot, Russia). Sulforhodamine B (SRB) for cytotoxicity studies was purchased from Sigma-Aldrich (USA). LHC-9 medium was a product of ThermoFisher Scientific, USA.

2.2. Synthesis and characterisation of polypeptide

Synthesis and characterisation of poly(L-glutamic acid-*co*-D-phenylalanine) (P(Glu-*co*-DPhe)) were carried out according to the previously published protocol (Zashikhina et al., 2019). Briefly, to the solution of mixed Glu(OBzl) and D-Phe N-carboxyanhydrides (NCAs) in 1,4-dioxane (4% wt), n-hexylamine was added. The molar ratio of Glu(OBzl)/D-Phe NCAs was equal to 6, while the NCAs/initiator molar ratio was 100. The reaction was proceeded for 4 days at 35 °C. The obtained polymer was precipitated with an excess of diethyl ether, and the precipitate was washed three times with diethyl ether, then dried.

The polymer molecular weights (M_n and M_w) and dispersity ($Đ$) were determined by size exclusion chromatography (SEC) using a Shimadzu LC-20 Prominence system equipped with a refractometric RID 10-A detector (Kyoto, Japan). The analysis was performed at 40 °C using 0.1 M LiBr in DMF as eluent (0.3 ml/min) and Styragel Column, HMW6E (7.8 mm × 300 mm, 15–20 μm bead size, Waters, Milford, MS, USA). Calculations were made using GPC LC Solutions software (Shimadzu, Kyoto, Japan) and preliminary

built calibration curve for poly(methyl methacrylate) standards with M_w 17,000–250,000 (≤ 1.14).

The deprotection of the copolymer was achieved using TFMSA/TFA mixture (1:10, *v/v*) at 25 °C for 4 h. After removing of the protective groups, the copolymer was precipitated with an excess of diethyl ether, then dissolved in DMF and purified *via* dialysis (MWCO 1000) sequentially against water for 48 h, 1 M NaCl for 24 h, and then again water for 48 h.

The composition of copolymers was calculated from ^{1}H NMR spectra. The spectra were recorded at 25 °C in DMSO-d_6 using a Bruker AC-400 NMR spectrometer (400 MHz) (Karlsruhe, Germany). For the calibration of the chemical shift scale of the NMR spectra the solvent peak at 2.52 ppm was used.

2.3. Preparation and characterisation of encapsulated forms

Empty nanoparticles (NPs) were formed due to self-assembly within the dialysis of polymer solution from DMF to water (see Section 2.2). The hydrodynamic characteristics of the nanoparticles (hydrodynamic diameter D_H, polydispersity index (PDI), and the ζ-potential) were analysed by dynamic light scattering (DLS) using a Zetasizer Nano-ZS Malvern (UK) equipped with a He–Ne laser at 633 nm at a scattering angle of 173°and 25 °C. For the storage of polymeric materials, the particles were freeze-dried and kept at 4 °C.

Preparation of the encapsulated forms of the hydrophobic drug paclitaxel (PTX) was carried out (PTX/NPs) as previously described (Levit et al. 2020). Briefly, 3 mL of a mixture of copolymer and paclitaxel (C_{NPs}=2 mg/mL, C_{PTX}=50 μg/mL) in DMSO was freeze-dried, then the precipitate was dispersed in H_2O using the ultrasonic probe UP 50H Hielscher Ultrasonics (Teltow, Germany). Unencapsulated paclitaxel was removed by centrifugation for 5 min at 3000 rpm. Thereafter, the supernatant containing the particles was collected, while the precipitate was dissolved in acetonitrile and analysed by HPLC.

Paclitaxel was quantified by reverse phase HPLC with UV detection ($\lambda = 237$ nm) using ZORBAX Eclipse XDB-C18 column (4.6 × 150 mm, 5 μm) from Agilent (CA, USA). The flow rate of the mobile phase was 0.5 mL/min, the volume of the injection loop was 20 μL. The analysis was performed under isocratic elution using 40% acetonitrile in deionised water (*v/v*). The retention time of paclitaxel was 7.8 min.

In the case of the doxorubicin (DOX) and irinotecan (Ir) encapsulation (Ir/NPs, DOX/NPs), an aliquot of a drug solution (1 mg/mL) in a buffer solution of 2-(N-morpholino)ethanesulfonic acid (MES, pH 6.0) was added to the NPs' suspension (2 mg/mL). Then, the mixture was dispersed under sonication and then left overnight at 4 °C for encapsulation and balancing the system. Unbound drug (DOX or Ir) was removed by dialysis using dialysis tubes with the 3500 MWCO membrane for 20 h.

Unbounded Ir and DOX were quantified by reverse phase HPLC with photometric detection at 356 and 480 nm, respectively, using the ZORBAX Eclipse XDB-C18 column (4.6 × 150 mm, 5 μm). The flow rate of the mobile phase was 0.5 ml/min, the volume of the injection loop was 20 μL. The isocratic elution mode was applied using the mixture of H_3PO_4 solution (pH 3.0) and acetonitrile (30:70, *v/v*). The retention times for Ir and DOX of paclitaxel were 4.2 and 5.5 min, respectively.

The concentration of drugs was determined according to a calibration curve preliminarily plotted using solutions of the test substance in the concentration range of 0.1–2.0 μg/mL.

Loading capacity (LC, μg/mg) and encapsulation efficacy (EE, wt%) were calculated using following equations:

$$LC = \frac{m_i - m_{un}}{m_{NP}} \quad (1)$$

$$EE = \frac{m_i - m_{un}}{m_i} \times 100\% \quad (2)$$

where m_i is the initial mass of the drug taken for loading (μg), m_{un} is the mass of the unencapsulated drug (μg), m_{NP} is the mass of nanoparticles taken for drug loading (mg).

The system containing two amphiphilic bases ((Ir + DOX)/NPs) was obtained by sequential addition of individual substances, followed by dispersion after the addition of each. For systems containing paclitaxel ((PTX + DOX)/NPs and (PTX + Ir)/NPs), PTX was encapsulated first, thereafter the resulting particles were dispersed in water and loaded with doxorubicin or irinotecan according to the methods described above. Encapsulation was carried out at a total load of substances ~25 μg/mg polymer, either at an equimolar ratio of drugs or at the ratio of $IC_{50\ (drug\ 1)}/IC_{50\ (drug\ 2)} = 1$.

The empty and drug-loaded nanoparticles were analysed by transmission electron microscopy (TEM) using a Jeol JEM-2100 transmission electron microscope (Kyoto, Japan). To prepare the samples for microscopy, the aqueous dispersions of polymer NPs (0.5 mg/mL) were dropped at the surface of the 300-mesh Cu grids covered with carbon and thin formvar film; the grids were dried and treated with a 2% (*w/v*)

uranyl acetate solution for 30–60 s, and after that left in air for 24 h at 22 °C. The calculation of the average particles' diameter from the TEM images was carried out with the use of ImageJ open software (the National Institute of Mental Health, Bethesda, MD, USA).

2.4. Release study

Drug release was studied under model physiological conditions (0.01 M PBS, pH 7.4 and 5.8, 37 °C). The dialysis method was used to study the release as previously described (Zashikhina et al. 2021). Briefly, 0.7 mL (inner solution) of NPs (2 mg) in 0.01 M phosphate-saline buffer (PBS) with pH 7.4 or 5.8 was placed into a dialysis tube (MWCO 3500). The tube was placed in 20 mL PBS (external solution) and was shaken at 37 °C. At predetermined time intervals, 4 mL of external solution was withdrawn for analysis and 4 mL of fresh PBS was added. Since the concentration of drugs in the withdrawn solution was extremely low for HPLC detection, the collected samples were lyophilised, then dissolved in 0.5 mL of mobile phase, and analysed as described above.

Mathematical dissolution models were applied for analysis of drugs release profiles. The linearisation of experimental release profiles was carried out with the following dissolution models: zero-order, first-order, Higuchi, Hixson–Crowell, Korsmeyer–Peppas, Baker–Lonsdale, Hopfenberg, Weibull, Gompertz, and Peppas–Sahlin (Bruschi 2015). The DDSolver add-in for Microsoft Excel (freely available software which was developed by Zhang Yong and colleagues from China Pharmaceutical University (Zhang et al. 2010) was used for this purpose. The correspondence of the release profile to a particular mathematical model was rated based on the values of the correlation coefficients. Various quantitative parameters of the models were also evaluated to find out the peculiarities of the drug release process.

2.5. Cell culture experiments

2.5.1. Cytotoxicity of NPs

The cytotoxicity of polymer NPs to normal cells was tested in human embryonic kidney cells (HEK 293), human retinal pigment epithelial cells (ARPE-19) and human bronchial epithelial cells (BEAS-2B) using Cell Titer-Blue (CTB) assay. HEK 293 and ARPE-19 were cultivated in Dulbecco's Modified Eagle's Medium (DMEM), while BEAS-2B was grown in LHC-9 medium; both media were supplemented with 10 vol% FBS and 1 vol% gentamicin. For the assay, 100 μL of a cell suspension in a culture medium containing 8×10^3 of cells was added into each well of a 96-well plate. The cells were cultured for 24 h in a humidified 5 vol% CO_2 atmosphere at 37 °C. After that, the medium was replaced with 200 μL of NPs dispersions in the culture medium ($n = 4$). The concentration of NPs was varied from 4 to 1000 μg/mL. Cells were incubated for 72 h and then the medium was removed, and 100 μL of 10% CTB stock solution in the culture medium was added per well. Cells were incubated with reagent in a CO_2 incubator for 2 h at 37 °C. The resorufin fluorescence was measured at 590 nm. The obtained data were normalised as a percentage of the control.

2.5.2. Inhibition of cancer cells

In the case of IC_{50} determination, the following single drug nanoformulations have been tested: DOX/NPs containing 23 μg DOX/mg of NPs, Ir/NPs containing 23 μg Ir/mg of NPs, and PTX/NPs containing 21 μg PTX/mg of NPs. The concentration of drugs used for testing was varied in the range of 0.01–5 μM for DOX (0.005–2.7 μg/mL), 0.08–110 μM for Ir (0.05–65 μg/mL) and 0.3–50 nM for PTX (0.25–43 ng/mL). Testing of dual drug delivery systems was carried out with the use of following nanoformulations: (PTX + DOX)/NPs containing 2.5 μg PTX and 23.4 μg DOX per mg of NPs, (PTX + Ir)/NPs containing 54.7 ng PTX and 25.1 μg Ir per mg of NPs, and (Ir + DOX)/NPs containing 25.1 μg Ir and 0.5 μg DOX per mg of NPs. The concentrations of drugs were varied from 0.05 × IC_{50} to 10 × IC_{50}, namely 0.01–2 μM for DOX, 0.325–65 μM for Ir and 0.35–70 nM for PTX.

HCT-116 cell line from ATCC was cultivated in DMEM supplemented with 10% FBS and 50 μg/mL gentamicin in all experiments. Cytotoxicity assay was performed in 96-well plates according to standard SRB protocol (Vichai and Kirtikara 2006) after 72 h of incubation with cytostatic drugs. This method is an anti-proliferative, metabolism independent assay and relies on a total amount of cellular protein in treated samples. The higher the cytotoxicity the lower the cellular protein abundance across the well after incubation with a cytotoxic agent. Cells for an experiment were seeded in a density of 5×10^3 cells per well and then the tested substances were added using the double dilutions method. Then the plates were placed at 37 °C and 5 vol% CO_2 conditions for 72 h. After incubation cells were fixed in 10% TCA for 10 min, then washed in dH_2O, and fixed cellular proteins stained with 0.4% SRB in 1% acetic acid for 10 min. Then

samples were washed in 1% acetic acid (*v/v*), dried and bound SRB was dissolved in 20 mM Tris-OH. Absorbance was measured at 570 nm using a Tecan SPARK spectrophotometer (Tecan, Switzerland), and cell viability was calculated as a ratio between tested and control wells ($n = 3$, outliers were detected and eliminated using the ROUT method with Q = 1% precision). The obtained data were normalised as a percentage of the control. Then sigmoidal curves and IC_{50} were constructed using GraphPad Prism software.

2.6. Statistical analysis

All data are presented as mean value ± SD ($n = 3$ for physicochemical experiments; $n = 3$–4 for biological experiments). The average diameter of NPs from TEM images was calculated as mean ± SD for the total number of analysed NPs equal to 15–30 per sample from three-five images. IC_{50} data for free drugs and their encapsulated formulations were analysed by two-way ANOVA using Instat GraphPad Software (San Diego, CA, USA). $p < 0.05$ was considered as statistically significant.

3. Results and discussion

3.1. Preparation and characterisation of encapsulated forms

The synthesis of P(Glu-co-DPhe) was performed *via* ring-opening polymerisation (ROP) of a mixture of α-amino acid NCAs as described in our previous study (Zashikhina et al. 2019). The composition of the synthesised copolymer was determined by ^{1}H NMR spectroscopy. According to calculations, the resulting polypeptide had the following composition: P((Glu(OBzl)$_{47}$-co-DPhe$_{11}$). The copolymer dispersity (Đ) determined by SEC was low and equal to 1.33. The hydrodynamic diameter and surface ζ-potential of empty P(Glu-*co*-DPhe) nanoparticles in 0.01 M PBS, pH 7.4, were 254 ± 30 nm and −43 ± 2 mV, respectively.

In the first step of preparing the encapsulated forms, the encapsulation of individual substances, namely irinotecan (Ir), doxorubicin (DOX) and paclitaxel (PTX) was developed and optimised. The encapsulated forms of the PTX (Figure 3a), which is a hydrophobic drug, were obtained by freeze-drying of the solution of copolymer and paclitaxel in DMSO followed by redispersion of the dried samples in aqueous media (deionised water or PBS) with short-time ultrasonication. Freezing the solution allows for the separation of the drug and polymer aggregates by solvent crystals. During freeze-drying, the hydrophobic drug interacts with the hydrophobic fragment of the polymer. Then as the solvent sublimates, the polymer shrinks to form solid NPs with hydrophilic segments of the polymer localised on the surface. When redispersed in an aqueous medium, NPs are stabilised by the presence of a hydrophilic shell minimising the energetically unfavourable contact of the hydrophobic content with water. Unencapsulated PTX was separated by ultracentrifugation.

The nanosystems obtained were characterised using dynamic light scattering (DLS). The hydrodynamic size (D_H), polydispersity index (PDI), and ζ-potential of empty particles, as well as encapsulated forms, are presented in Table 1. The size of particles containing encapsulated PTX was found to be smaller than that of the empty particles. This reduction in size is probably caused by a compaction of the hydrophobic core of NPs when paclitaxel is included in it.

For irinotecan (Ir) and doxorubicin (DOX) which are amphiphilic bases, it is assumed that the binding with the polymer carrier occurs through electrostatic interactions. Initially, two techniques were tested for the formation of encapsulated forms of Ir and DOX: (1) the same technique applied for PTX and (2) a modified technique in which borate buffer solution (pH 9.4) was added to the mixture. In the latter case, the intention was to bind HCl and convert the commercial hydrochloride salts into their base forms. Both of these approaches assumed encapsulation of the substances through predominantly hydrophobic interactions, as in the case of paclitaxel. However, in both cases, relatively low encapsulation efficiency (<60%) was achieved and, at the same time, strong particle aggregation occurred.

To optimise the encapsulation protocol and achieve a stable dispersion of the loaded particles, a third technique was tested for encapsulating these substances (Figure 3b,c). In this approach, polymer nanoparticles were initially formed in water, and then a solution of a drug (Ir or DOX) in a MES buffer solution (pH 6.0) was added. The mixture prepared was ultrasonicated and the unbound drug was removed by dialysis. The calculated characteristics of the encapsulated forms are presented in Table 1. High encapsulation efficiency (*EE*) values (≥79%) were achieved for both systems. Moreover, the aqueous dispersions of the obtained encapsulated systems exhibited physicochemical characteristics similar to those of the empty nanoparticles (Table 1) and remained stable against aggregation for at least one week. In comparison to PTX, the encapsulation of doxorubicin and irinotecan

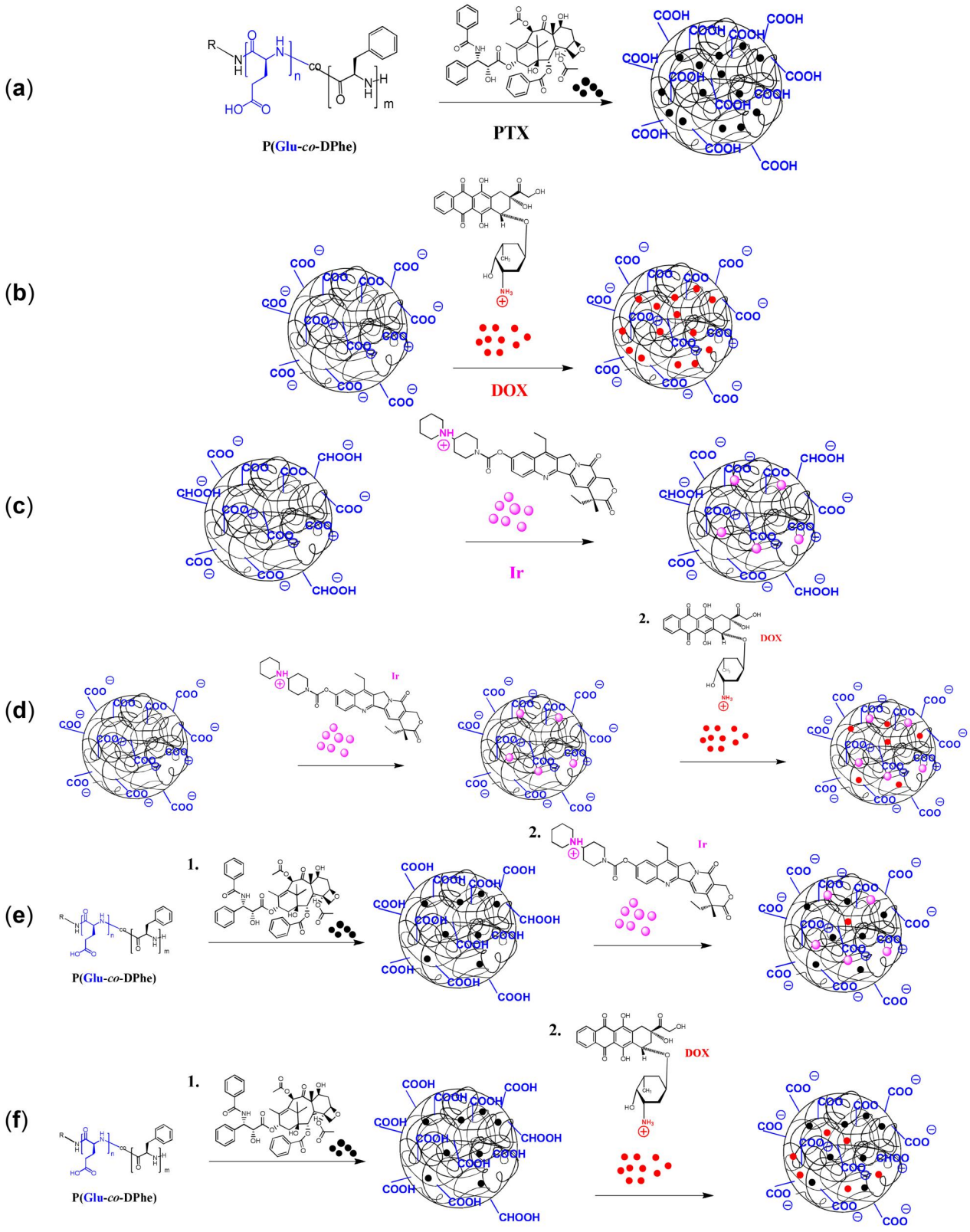

Figure 3. Scheme for the preparation of encapsulated forms of individual drug substances: (a) paclitaxel (PTX/NPs), (b) doxorubicin (DOX/NPs), (c) irinotecan (Ir/NPs), as well as co-encapsulated forms containing two substances: (d) irinotecan with doxorubicin ((Ir + DOX)/NPs), (e) paclitaxel with irinotecan ((PTX + Ir)/NPs) and (f) doxorubicin with paclitaxel ((DOX + PTX)/NPs).

Table 1. Physicochemical characteristics of dispersions of empty nanoparticles and single-drug encapsulated forms (determined in 0.01 M PBS, pH 7.4; $n = 3$).

Nanoformulation	*LC*[a] (μg/mg of NPs)	*EE* (%)	D_H[b](nm)	*PDI*[b]	ζ-*potential*[c] (mV)
Empty NPs	–	–	254 ± 3	0.20 ± 0.02	−43 ± 2
PTX/NPs	21 ± 1	83 ± 3	182 ± 1	0.10 ± 0.01	−30 ± 2
Ir/NPs	23 ± 1	79 ± 3	250 ± 4	0.20 ± 0.02	−49 ± 4
DOX/NPs	23 ± 1	91 ± 4	226 ± 4	0.18 ± 0.02	−48 ± 4

LC: loading capacity; EE: encapsulation efficacy; D_H: hydrodynamic diameter; PDI: index of polydispersity; NPs: nanoparticles; PTX: paclitaxel; Ir: irinotecan; DOX: doxorubicin.
Determined by.
[a]HPLC analysis.
[b]Dynamic light scattering.
[c]Electrophoretic light scattering;.

Table 2. Physicochemical characteristics of dispersions of encapsulated dual-drug nanoformulations (determined in 0.01 M PBS, pH 7.4; $n = 3$).

Nanoformulation	Drug	*LC*[a] (μg/mg of NPs)	*EE* (%)	D_H[b](nm)	*PDI*[b]	ζ-*potential*[c] (mV)
(PTX + Ir)/NPs	PTX	11.4 ± 0.5	82 ± 4	146 ± 1	0.10 ± 0.01	−32 ± 5
	Ir	10.0 ± 0.2	91 ± 2			
(PTX + DOX)/NPs	PTX	11.2 ± 0.1	75 ± 1	162 ± 2	0.11 ± 0.02	−36 ± 4
	DOX	9.0 ± 0.1	88 ± 2			
(Ir + DOX)/NPs	Ir	12.3 ± 0.2	92 ± 2	248 ± 4	0.19 ± 0.02	−42 ± 2
	DOX	11.0 ± 0.3	95 ± 3			

LC: loading capacity; EE: encapsulation efficacy; D_H: hydrodynamic diameter; PDI: index of polydispersity; NPs: nanoparticles; PTX: paclitaxel; Ir: irinotecan; DOX: doxorubicin.
Determined by.
[a]HPLC analysis.
[b]Dynamic light scattering.
[c]Electrophoretic light scattering.

did not affect the hydrodynamic diameter of the particles. A similar result for DOX-loaded polypeptide nanogels consisting of block-copolymer with poly(glutamic acid) as one of the blocks was observed elsewhere (Desale et al. 2015).

At the next step, methods for co-encapsulation of two drugs in one system were developed. A system containing two amphiphilic bases (irinotecan and doxorubicin) was obtained by sequentially adding individual substances, followed by ultrasonic dispersion after the addition of each (Figure 3d). For the systems containing PTX, PTX was encapsulated first as described earlier, followed by dispersing the formed particles in water and encapsulation of doxorubicin or irinotecan (Figure 3e,f) according to the procedure described above. Two substances were encapsulated at an initial total loading of 25 μg/mg of the polymer at an equimolar ratio of the two individual drugs. As can be seen from Table 2, the co-encapsulation of hydrophobic PTX and amphiphilic Ir/DOX demonstrated the same trends as the loading of the single drugs. In particular, the encapsulation efficiency for hydrophobic PTX and amphiphilic Ir was lower than for DOX. Furthermore, similar to single-drug encapsulated systems, the dual-drug systems loaded with PTX favoured the considerable compaction of the nanoparticles (see Tables 1 and 2). Similar to the single-drug encapsulation co-loading the amphiphilic drugs (Ir + DOX) did not affect the hydrodynamic diameter of the nanoparticles.

The hydrodynamic diameter of both single and dual drug formulations did not exceed 250 nm with a PDI of less than 0.2. Thus, the characteristics of the obtained delivery systems are acceptable for parenteral administration meeting the criteria for soft nanomaterials with a $D_H < 300$ nm (Williams et al. 2003, Ferrari et al. 2018) and PDI < 0.3 (Xu et al. 2022).

Encapsulation efficacy depends on various factors, including the nature of the polymer, reactive functionality, the type of NPs, the method for preparation of formulation as well as the type of interaction between drug and polymer. For example, lower encapsulation efficiency for hydrophobic drugs has been observed in the literature for other delivery systems. When co-encapsulated in liposomes, high efficiency has been described for amphiphilic bases such as DOX, Ir or epirubicin (>70%), while for hydrophobic substance erlotinib it was much lower (40%) (Morton et al. 2014, Yang et al. 2014, Liu et al. 2019). In turn, when encapsulation was carried out in PLA or PLGA-based polymer particles, loading depended on the composition of the particle and the mixture being encapsulated. For example, single-drug-loaded PLGA-based nanoparticles allowed the encapsulation efficiency of over 80%, while the *EE* of co-loaded systems was markedly decreased (35–50%) (Xiao et al. 2015a). The

encapsulation efficiency of hydrophobic drugs increased with an increase in the hydrophobicity of the particles (Do et al. 2018).

In our study, similar to individual substances, dual-drug loading also resulted in high encapsulation efficiencies (the loading of both components was $\geq$ 75%) (Table 2). This suggests the involvement of different mechanisms of interaction between the polymer and the drug. Similar highly efficient co-loading was previously also observed in other studies. For example, the co-encapsulation of hydrophobic 7-allylamino-17-demethoxygeldanamycin (17-AAG) and paclitaxel in mixed polymeric micelles were performed with an *EE* of about 95% for PTX and 90% for 17-AAG (Katragadda et al. 2011).

In addition, the obtained empty and some of the drug loaded NPs were analysed by transmission electron microscopy (TEM). The TEM images (Figure 4), revealed that all NPs have a spherical shape and rather small sizes in the dry state. In particular, the average diameter of empty nanoparticles in the dry state was 65 ± 19 nm. In turn, the average diameters of the single-loaded nanoformulations, namely PTX/NPs and DOX/NPs, were 45 ± 16 and 91 ± 29 nm for PTX, respectively, and 85 ± 15 nm for the dual-drug (PTX + DOX)/NPs formulation. The difference in hydrodynamic diameter and size in the dry state is known for soft nanoparticles attributed to the presence of a solvate shell and electrostatic repulsion for charged polymers (Marsden et al. 2010, Moughton et al. 2011, Zashikhina et al. 2019). Thus, the formed nanoparticles are loose nanogels in an aqueous medium and undergoes significant compaction upon drying.

3.2. Release study

One of the most important characteristics in the development of drug delivery systems is the rate of the encapsulated drug release, since the release patterns determines their prolonged action. Drug release was studied under model physiological conditions (0.01 M PBS, 37 °C), simulating the environment in the bloodstream (pH 7.4), and the tumour microenvironment (pH 5.8). The dialysis method was used to study the

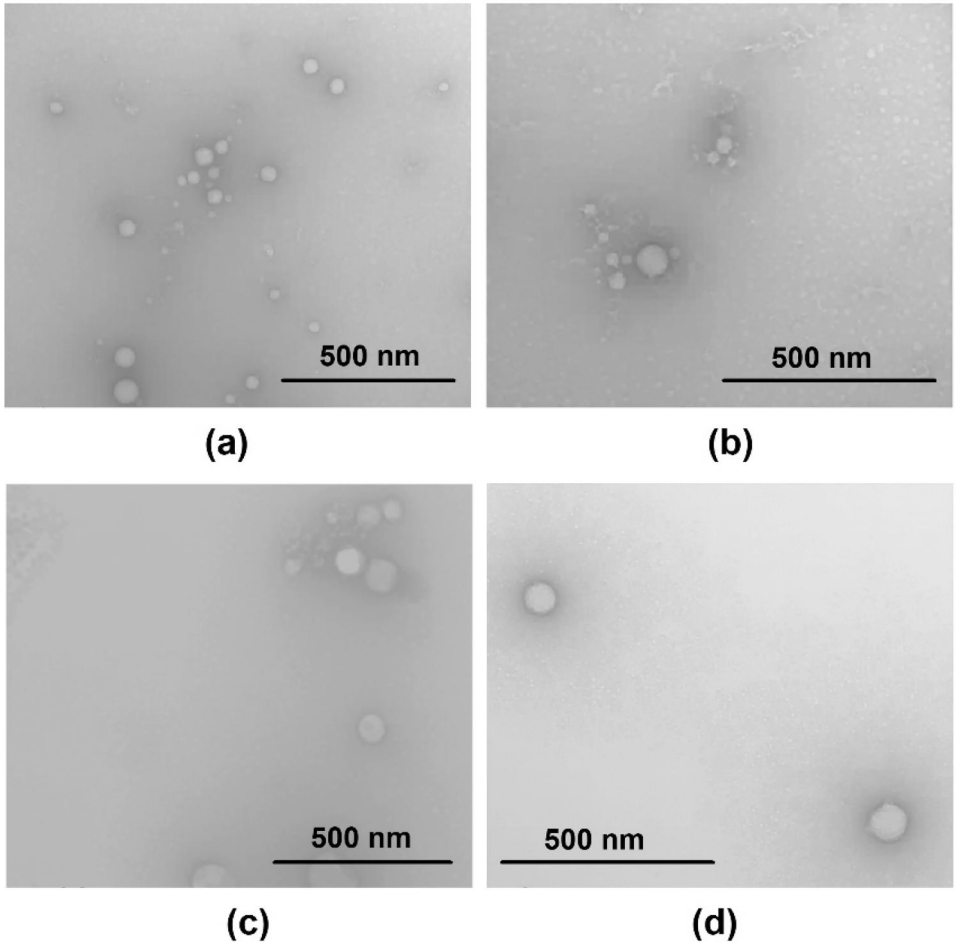

Figure 4. TEM images of empty P(Glu-*co*-DPhe)-based nanoparticles, and single- and dual-drug nanoformulations (uranyl acetate staining): empty NPs (a), DOX/NPs (b), PTX/NPs (c) and (DOX + PTX)/NPs (d).

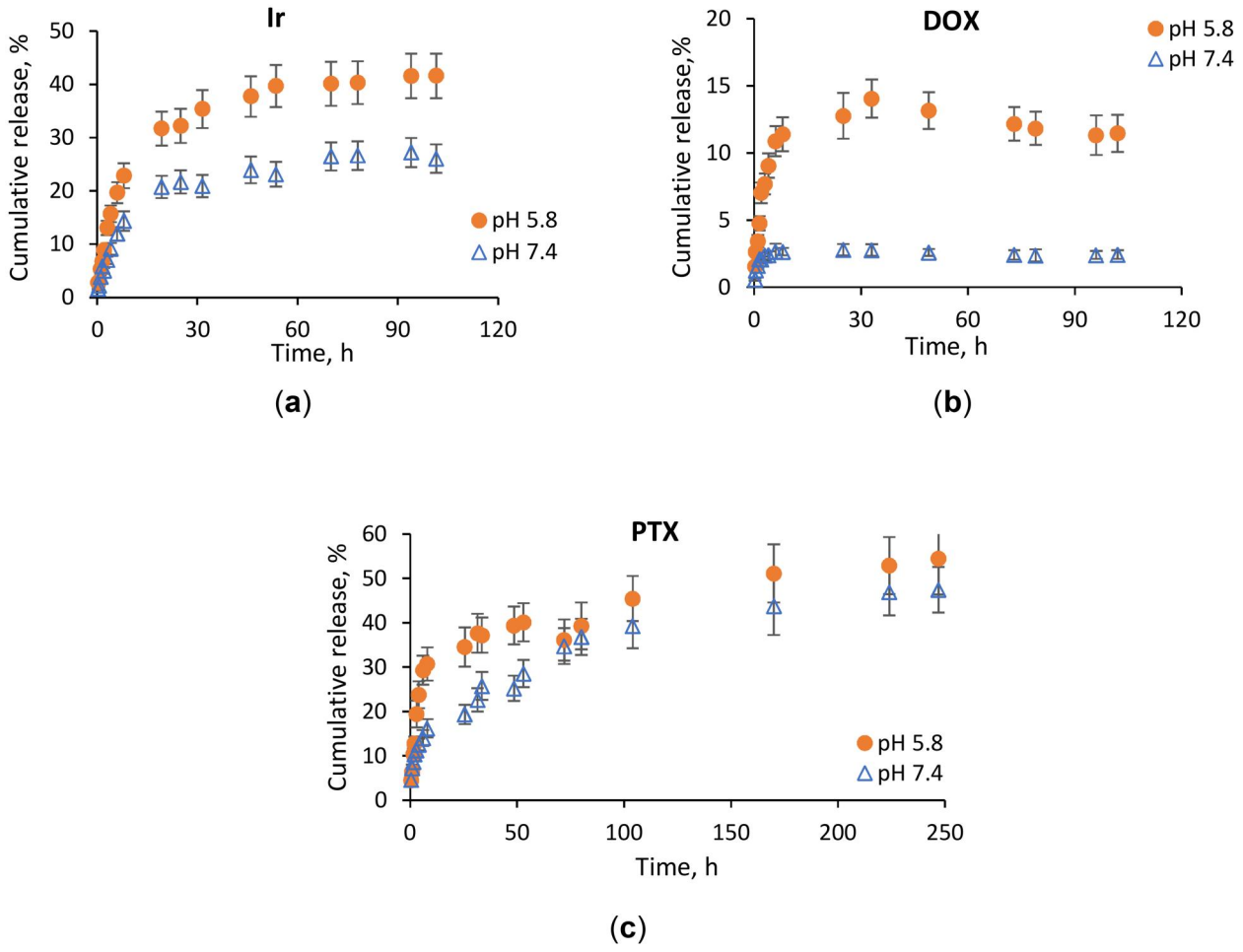

Figure 5. Cumulative release profiles of irinotecan (Ir; LC = 23 μg/mg of NPs) (a), doxorubicin (DOX; LC = 23 μg/mg of NPs) (b), and paclitaxel (PTX; LC = 21 μg/mg of NPs) (c) from polymer particles based on P(Glu-*co*-DPhe). *Conditions:* 37 °C, 0.01 M PBS, pH 7.4 and 5.8.

release (Levit et al., 2018). The concentration of substances was determined by reverse phase HPLC with UV or photometric detection (Section 2.3). The release profiles of irinotecan, doxorubicin, and paclitaxel under model conditions are shown in Figure 5.

In all cases, the most rapid release was observed within 8 h of incubation. The results revealed a rather faster release of drugs at a more acidic pH compared to physiological one. Specifically, during the initial 8 h at pH 5.8, 23 and 31% of the encapsulated irinotecan and paclitaxel were released, respectively (Figure 5a,c). For comparison, during the same period of time, at pH 7.4 only 14% of Ir and 16% of PTX were released. For the system containing doxorubicin, the slowest release of the substance was observed: in the first 8 h at pH 5.8, 11% of the encapsulated DOX was released, while about 3% of the drug was released at pH 7.4 (Figure 5b). After this time, no further DOX release was detected under model conditions.

The release rate significantly slowed down after 24 h of incubation. For instance, the release of irinotecan increased from 22 to 27% when incubated from 24 to 72 h at pH 7.4, reaching a maximum and remaining constant thereafter (up to 200 h). Similar results were obtained for this system at pH 5.8, however, the release rate was higher with the release accumulating from 32 to 40%. A similar trend was observed for PTX – the release rate slowed down after 24 h of incubation. However, unlike amphiphilic bases, the gradual release of PTX was occurred over a long period of time, and even after 100 h of incubation a slow release was observed. For example, the amount of paclitaxel released from 25 to 250 h increased from 19 to 47% at pH 7.4 and from 35 to 54% at pH 5.8. It is worth noting that the release curves exhibit a similar trend for both pH values starting from 100 h of the experiment. This may be attributed to the fact that in the initial hours of the experiment, the particle structure, which

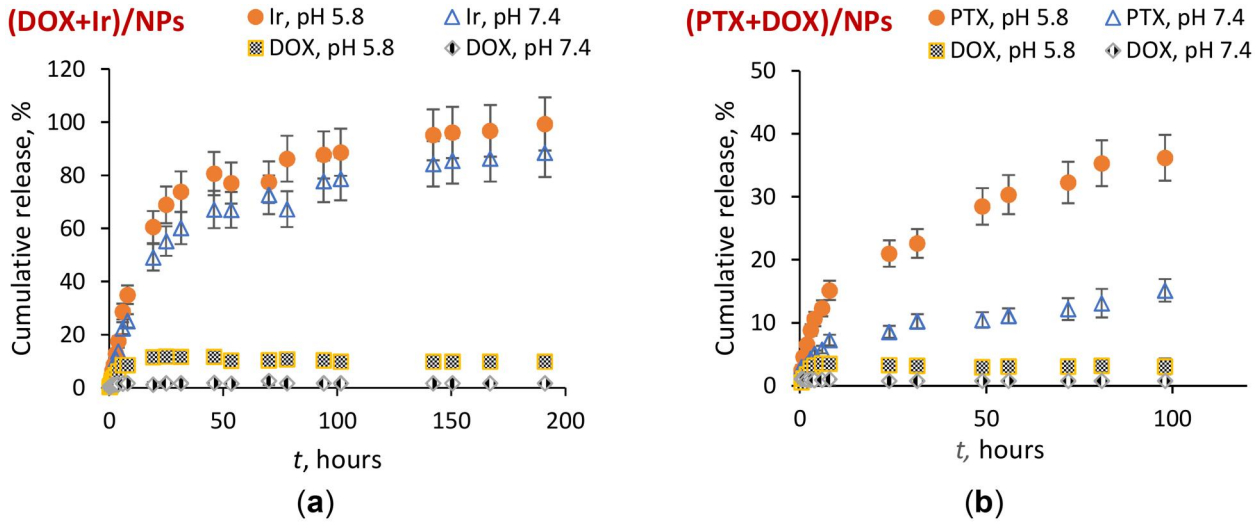

Figure 6. Cumulative release profiles of irinotecan (Ir), doxorubicin (DOX), and paclitaxel (PTX) from nanoparticles based on P(Glu-co-DPhe), loaded with Ir + DOX (LCt = 23.3 μg/mg of NPs) (a), and DOX + PTX (LCt = 20.2 μg/mg of NPs) (b). *Conditions:* 37 °C, 0.01 M PBS, pH 7.4 and 5.8.

appears to differ at different pH, affects the release. After the release of PTX from the surface layer, its release is determined by hydrophobic interactions with the hydrophobic core, which do not depend on the acidity of the solution.

In general, the release patterns of individual substances from dual drug-loaded systems were similar to those of systems containing one drug (Figure 6). In particular, the release was faster at acidic pH. However, several features are worth noting. For instance, in the case of the delivery system containing two amphiphilic bases (DOX and Ir), the release of irinotecan reached 100% within 200 h (Figure 6a) whereas in the system containing only irinotecan, where the maximum amount of irinotecan released was 40%. At the same time, the release of doxorubicin from this system showed values similar to those of the system containing individual doxorubicin. These results suggest that the particle structure during co-encapsulation differs from that of particles loaded with individual drug. It can be assumed that in the presence of a competing base (doxorubicin), irinotecan binds less strongly to the polymer.

According to the literature, when Ir and DOX were co-encapsulated in liposomes (Liu et al. 2019), the release profile of both substances in PBS was almost equal and achieved about 40% in 3 days. This difference in the behaviour of the encapsulated substances is apparently associated with a different interaction with the nanocarrier. In the case of liposomes, the drug is located in the inner water core of the liposome, while in this research the retention of the amphiphilic substances is based on ionic and hydrophobic interactions within the polymer matrix.

For the system containing co-encapsulated doxorubicin and paclitaxel (Figure 6b), a slower release of doxorubicin from particles was observed compared to the system containing individual doxorubicin (Figure 6b). This feature may be attributed with a lower loading of doxorubicin into such particles, and, as a result, less amount of doxorubicin on the surface of the particles weakly retained due to the ionic interactions with the polymer matrix. The release profile of paclitaxel was similar to that of the pure paclitaxel system; however, slower release values were observed at the same pH. This can probably due to the binding of doxorubicin causes a change in the particle structure and contributes to the changes in hydrophobic interactions with the particle hydrophobic core. In addition, it is worth mentioning that the influence of co-encapsulation with doxorubicin affects the release of PTX to a greater extent at low pH value.

The release rate depends strongly on the drug and carrier nature. As for the co-loaded liposome system, amphiphilic base erlotinib, located in the exterior lipid bilayer membrane compartment, was released faster (60% in 24 h) than doxorubicin (20%), enclosed in the hydrophilic core of the liposomes (PBS, pH 7.4, 37 °C) (Batist et al. 2009). For dual-loaded PLGA-PEG-based nanoparticles, hydrophobic PTX was observed to be released sustainably over several days without burst release at early time points at both pH 7.4 and 6.5. The release profiles were similar for both pH, and the systems do not appear to be greatly affected by pH,

while PTX has been greater retained than lonidamine (Milane et al. 2011). It was demonstrated that in 72 h 100% of lonidamine have been released at both pH 7.4 and 6.5, whereas only 52% of PTX were released at 7.4 and 57% at pH 6.5. The co-encapsulated systems also had similar release profiles as the single-loaded ones (Milane et al. 2011).

In our study for all tested systems, the release rate of drugs at a lower pH was faster, which will contribute to the accumulation of the drug in the tumour site. It is assumed, that the release of drug molecules *in vivo* will occur faster than in the considered model experiment, which is associated with the effect of plasma components that affect the destruction of the particle, as well as the presence of enzymes that catalyse the process of polypeptide degradation.

In order to analyse the mechanism of drugs release from prepared formulations we have applied a number of mathematical models. Figure 7 presents the comparison of correlation coefficients obtained by approximation by the mathematical models and the visualisation of the most important parameters.

The analysis of single-drug formulations showed that the most controllable release is observed in the case of PTX, which is the most hydrophobic drug among the studied. The fitting was less successful for more hydrophilic Ir, and the worst correlation coefficients were observed in the case of DOX release. Correlation coefficients obtained by approximation of release of PTX, Ir and DOX to Higuchi and Baker-Lonsdale models were higher than those obtained by approximation to Hixon-Crowell and Hopfenberg models (Figure 7a–c). Thus, drugs release from formulations under study might be considered as diffusion-controlled transport of drugs from spherical particles. This is in good correlation with *n* parameters, obtained from Korsmeyer-Peppas model (Figure 7d), the values of which (0.10–0.34) allow to assume that Fickian

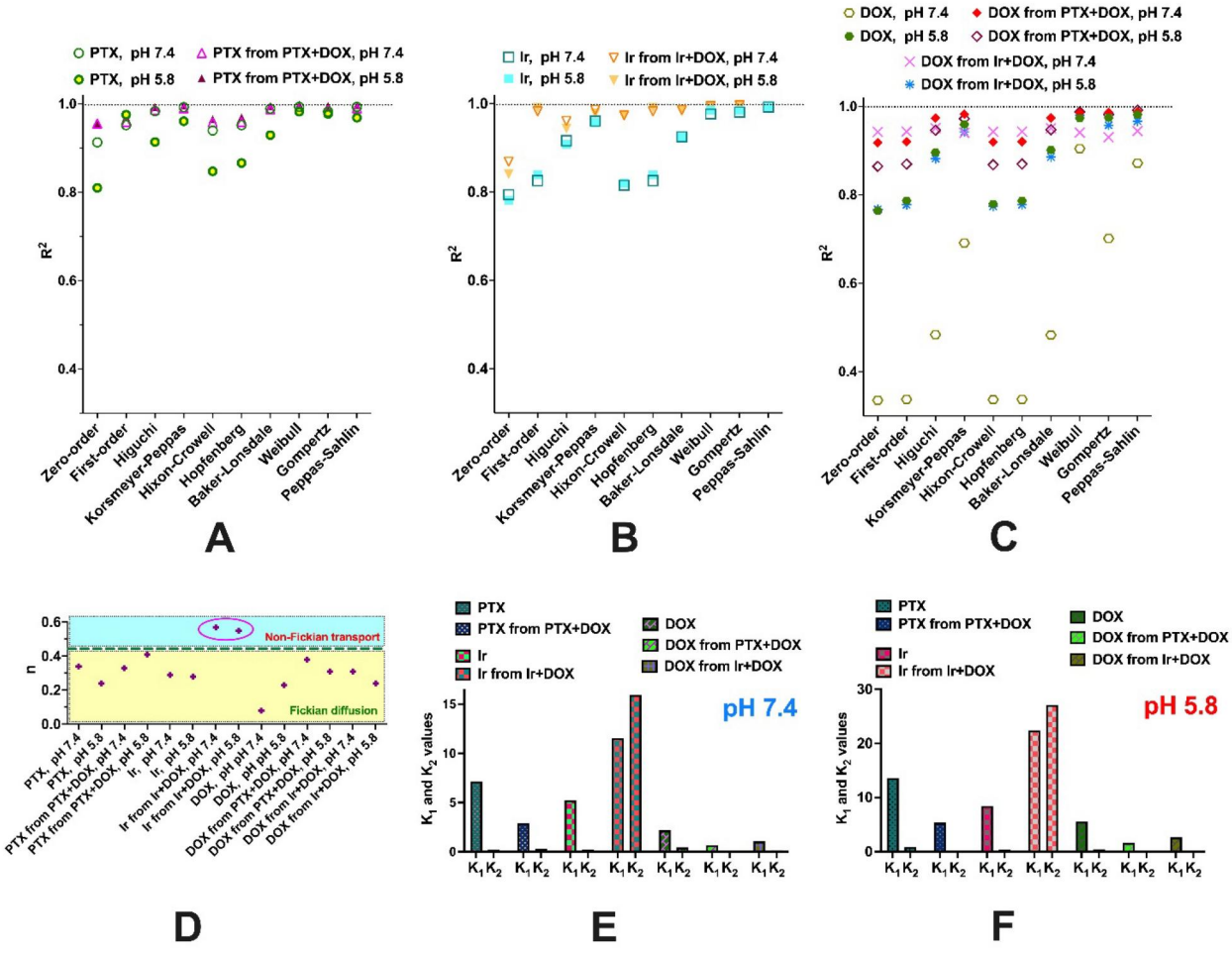

Figure 7. Results of approximation of the drug release profiles with application of various mathematical models. Comparison of correlation coefficients for single- and dual-drug formulations: (a) – PTX; (b) – Ir; (c) – DOX; Comparison of *n* parameter obtained from Korsemeyer-Peppas model for different systems under investigation (d); Comparison of K_1 and K_2 parameters, obtained from Peppas-Sahlin model and showing the impact of diffusion and polymer relaxation, respectively: (e) – for release at pH 7.4; (f) – for release at pH 5.8.

diffusion is the mechanism, which controls the drug release in the systems under investigation. Considering the effect of pH one can observe that in the case of PTX the release is more controllable at neutral pH, while much better correlations were found for the DOX release at pH 5.8. No effect of pH on correlation coefficients was observed in the case of Ir release modelling.

The reason for unsatisfactory approximation of DOX release with all models could be the more complicated mechanism of this drug release. It appears that DOX transport within designed particles is affected by strong drug-polymer interactions, which greatly decrease the DOX diffusion coefficient.

Parametric models (Weibul, Gomperz, and Peppas-Sahlin) showed very nice approximation to all drug release profiles. Thus, the obtained parameters of these models could be considered as relevant and used for drug release mechanism analysis. Nearly all release curves under study were well-fitted with the Gomperz model, which describes the immediate release of drugs with good solubility. The β parameter obtained from this model expresses the dissolution rate. This rate was found to be similar in the case of PTX (0.57 and 0.51 at pH 7.4 and 5.8, respectively) and Ir (0.39 and 0.53 at pH 7.4 and 5.8, respectively), but was much less in the case of DOX (0.05 and 0.24 at pH 7.4 and 5.8, respectively).

Of interest was the comparison of K_1 and K_2 parameters in the Peppas-Sahlin model, which are responsible for diffusion and polymer relaxation impacts on drug release, correspondingly (Bruschi 2015). One can observe (Figure 7e,f) that in single-drug formulations the diffusion (K_1) had a greater influence on the drug release than polymer relaxation (K_2).

The Weibull model is not associated with any mechanism of release but allows for evaluation of the time dependence parameter α and release curve progression parameter β. All β values were found to be below 1, which indicates the high initial slope of the exponential curve that is a characteristic of fast dissolving drugs. The time dependence parameter α was found to be the greatest in the case of DOX release. Interestingly, that this parameter was always less in the case of pH 5.8 as compared to pH 7.4 (PTX: 14.6/5.37; Ir: 11.41/5.71; DOX: 45.30/15.60), which reveals the more rapid release of all drugs at acidic conditions.

The comparison of single-drug and dual-drug formulations showed that correlation coefficients in the latter case are significantly higher. This shows that the release of a drug from particles containing another co-encapsulated drug is different from the release of a single drug. In the case of Ir, the co-encapsulation with DOX has led to a change of n parameter values in the Korsmeyer-Peppas model (Figure 7d). It is known that n values equal or below 0.45 are characteristic for Fickian transport, when diffusion is slow and determines the release process (Bruschi 2015). When n is above 0.45, the process can be categorised as non-Fickian diffusion, in which both diffusion and polymer relaxation play their important roles. This change of mechanism is also supported by similar values of K_1 and K_2 parameters derived from the Peppas-Sahlin model (Figure 7e,f). Such change of Ir release mechanism could be explained by increasing of particles density caused by polymer-DOX-polymer interactions within hydrophobic parts of macromolecules. Such density growth leads in turn to the change of Ir localisation within the particles. It appears that Ir is pushed to more hydrophilic surface regions of the particles. As a result, more rapid Ir release occurs and this process is affected by polymer relaxation, namely, swelling of hydrophilic parts of macromolecules.

At the same time, no change of n parameter values in the Korsmeyer-Peppas model was observed in the case of more hydrophobic PTX and DOX release from double-drug formulations. In these cases, the slow diffusion takes place and determines the rate of release. However, it is notable that release of these drugs become more controllable in double-drug formulations (Figure 7(a,c)). The possible reason for such effect is the possible structuring and compactization of polymer particles caused by the addition of the low-molecular hydrophobic drug. Such structuring of polymer molecules leads to more controllable diffusion. The discussed effect is most evident in the case of DOX release, when it was co-encapsulated with PTX (Figure 7c).

Overall, it could be concluded that the main mechanism of drug release from the designed nanoparticles is diffusion. Co-encapsulation of two drugs results in noticeable change of diffusion process. It could be supposed that after such co-encapsulation more hydrophobic drugs act as non-covalent cross-linkers, leading to the increase of particles density with hydrophobic regions of the particles. In the case of more hydrophilic drug (Ir) co-encapsulation with more hydrophobic one (DOX) this leads to pushing of the hydrophilic one out to the hydrophilic regions of the particles. In such a variant release of hydrophilic drugs began to be affected by polymer swelling. When more hydrophobic drugs (DOX + PTX) are co-encapsulated together, such non-covalent cross-linking result in

altering of drug diffusion rate and as a result of release rate as well.

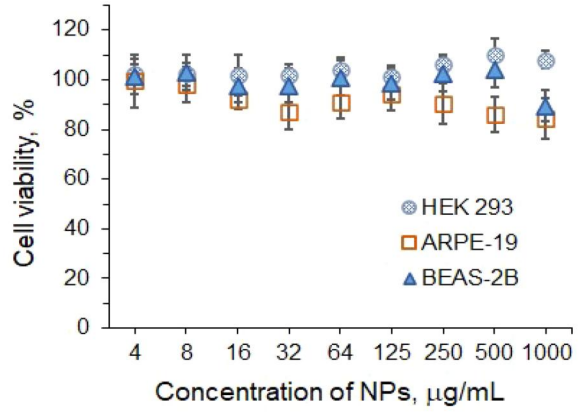

Figure 8. Viability of various normal cells in the presence of P(Glu-*co*-DPhe) nanoparticles tested in the concentration range of 4–1000 μg/mL (HEK 293: human embryonic kidney cells; ARPE-19: human retinal pigment epithelial cells; BEAS-2B: human bronchial epithelial cells; 72 h; $n = 4$).

3.3. In vitro biological evaluation

3.3.1. Cytotoxicity of NPs to normal cells

In vitro cytotoxicity of NPs was examined in the concentrtion range of 4–1000 μg/mL for 72 h using a set of normal cells such as HEK 293, ARPE-19 and BEAS-2B (Figure 8). In all cases, cell viability exceeded 80% over the entire concentration range. According to ISO EN 10993–5 protocol's criteria, a cytotoxic effect is recognised as a reduction in cell viability of more than 30% (ISO 10993-5 2009, Podgórski et al. 2022). Thus, the investigated NPs can be considered non-toxic to normal cells.

3.3.2. Cancer cells inhibition by single and dual-drug formulations

In the first stage, *in vitro* anti-cancer activity of free and encapsulated into the polymer particles antitumor drugs – doxorubicin (DOX), irinotecan (Ir), and paclitaxel (PTX), was evaluated. Cytotoxicity was studied using the HCT-116 colon cancer cell line, which is sensitive to all three drugs studied. The incubation time

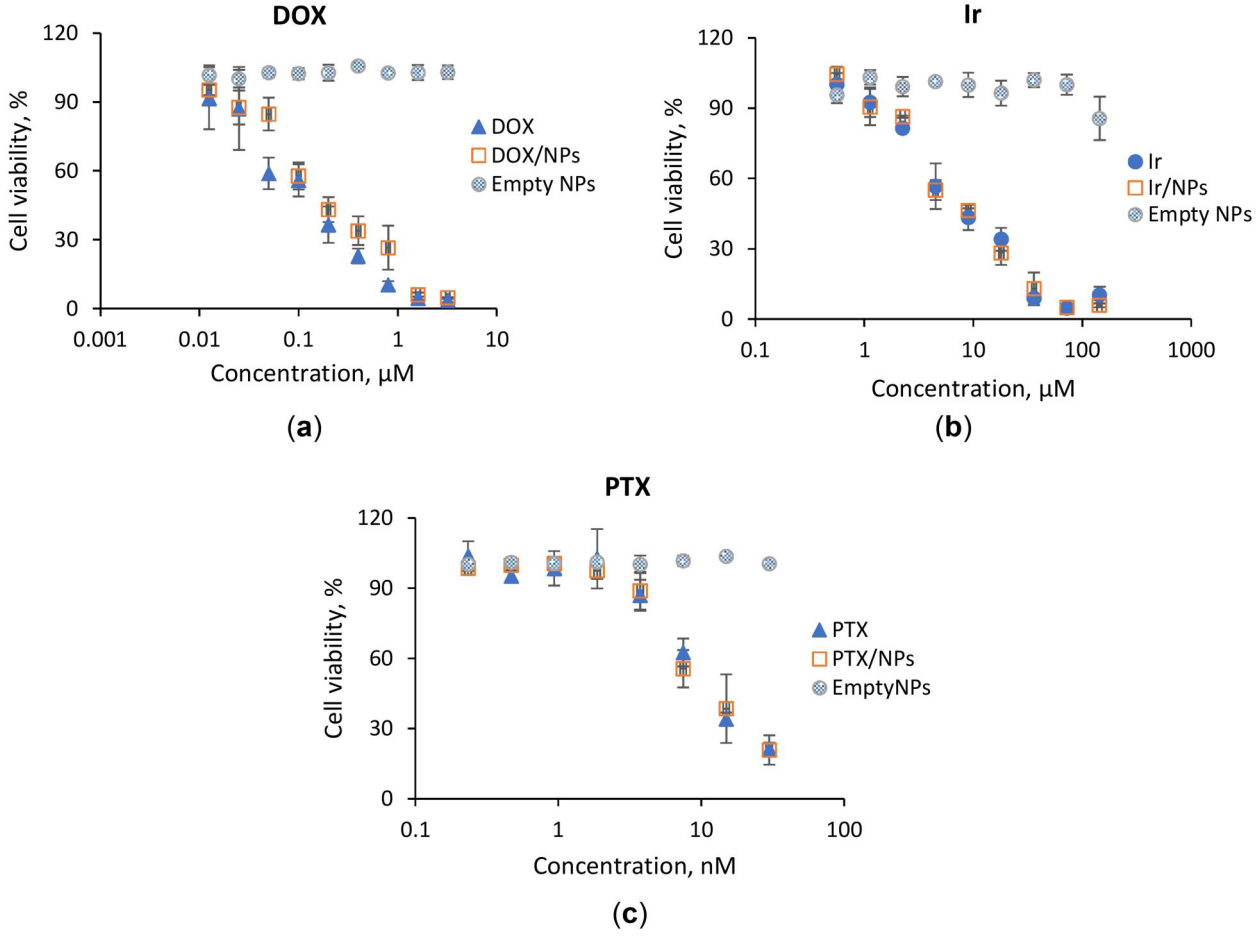

Figure 9. Viability of the colon cancer cells (HCT-116 cell line) incubated with empty nanoparticles, as well as with free and encapsulated drugs – doxorubicin (DOX; LC = 23 μg/mg of NPs) (a), irinotecan (Ir; LC = 23 μg/mg of NPs) (b) and paclitaxel (PTX; LC = 21 μg/mg of NPs) (c) (72 h, $n = 3$).

was 72 h. The viability of cells in the presence of various forms of anti-tumour drugs, as well as empty nanoparticles at concentrations corresponding to the concentration of particles of encapsulated forms, is shown in Figure 9. The obtained IC_{50} values found for the free substances and their encapsulated forms are presented in Table 3.

No loss of the *in vitro* anti-cancer activity of the drug due to its encapsulation was observed. Thus, the IC_{50} values for the free and encapsulated forms of anti-tumour drugs are almost the same (within the margin of error), while empty particles were found to be non-toxic in all concentration ranges studied (up to 5 mg/mL). The statistical analysis of IC_{50} values for corresponding free and encapsulated drug revealed no statistical significance in these values ($0.05 < p < 0.1$).

Table 3. Cytotoxicity of free drugs and their single-drug nanoformulations to colon cancer cells (HCT-116 cell line, 72 h, $n = 3$).

Sample	IC_{50}[a]
DOX	0.12 ± 0.06 μM
DOX/NPs	0.19 ± 0.11 μM
Ir	5.48 ± 2.10 μM
Ir/NPs	6.49 ± 2.54 μM
PTX	8.19 ± 2.54 nM
PTX/NPs	6.95 ± 0.72 nM

NPs: nanoparticles; PTX: paclitaxel; Ir: irinotecan; DOX: doxorubicin.
aNo statistically significant difference was found for IC_{50} values of corresponding free and encapsulated drug ($0.05 < p < 0.1$).

After that, to evaluate the joint action of drugs, the cytotoxicity of the combination of two free drugs (pairwise (DOX + Ir), (DOX + PTX) and (Ir + PTX)) was studied. For this, the concentration of one drug was fixed, while the concentration of the second substance was varied. Based on the data obtained, isobolograms were plotted to assess the synergy or antagonism of the selected pair (Roell et al. 2017) (Figure 10). The (DOX + Ir) combination exhibited a synergistic drug effect, while a pair of PTX-containing anti-tumour drugs ((Ir + PTX) and (DOX + PTX)) showed antagonism (Figure 10).

The joint action of two encapsulated drugs was analysed both for a mixture of two single-drug formulations (e.g. Ir/NPs + DOX/NPs), and for dual-drug co-encapsulated system (e.g. (Ir + DOX)/NPs). In the first case, particles were taken with the same drug loading content, but in different proportions, so that the total

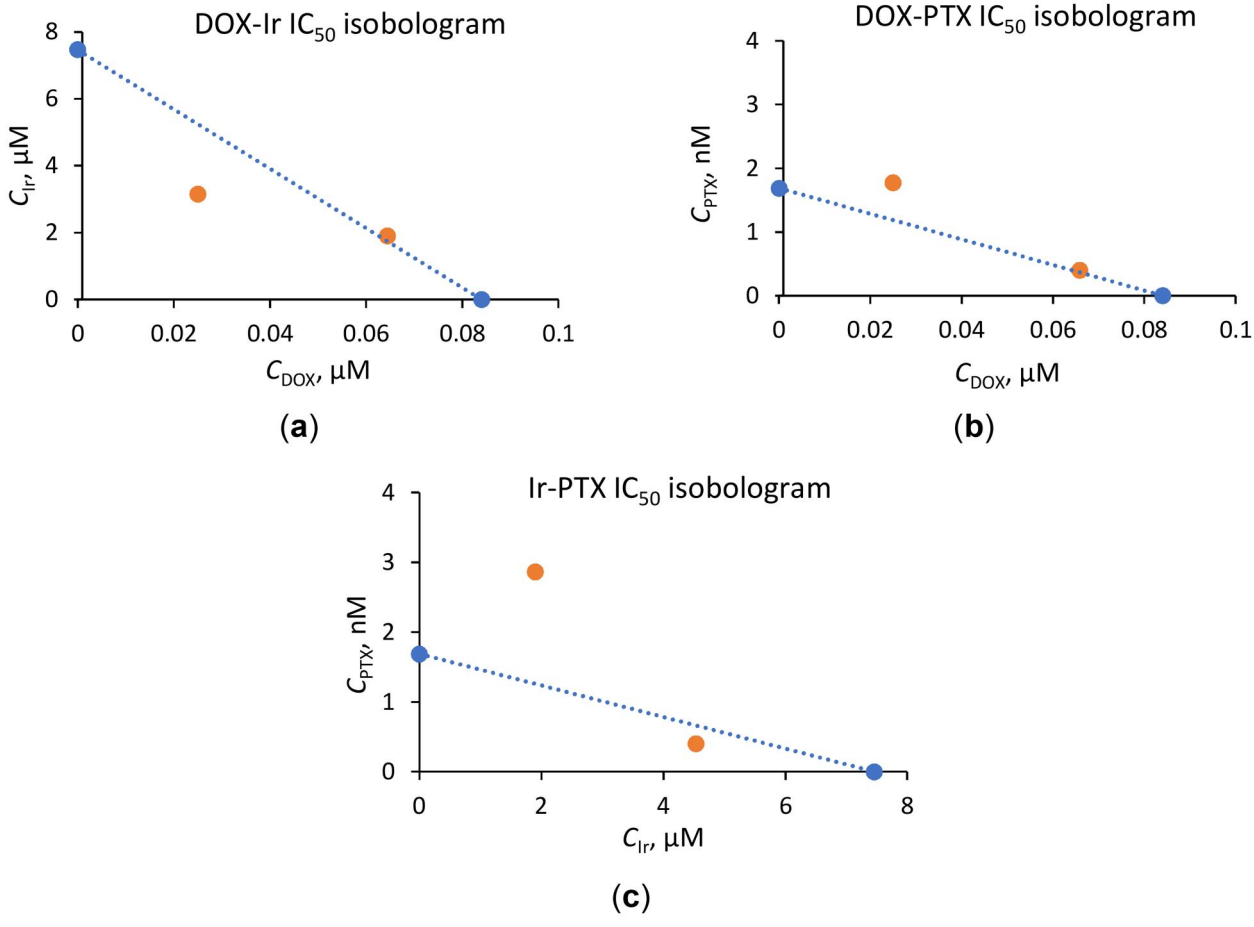

Figure 10. Isobolograms plotted for a combination of free chemotherapeutics (HCT-116 cells, 72 h): (a) irinotecan and doxorubicin (Ir + DOX), (b) doxorubicin and paclitaxel (DOX + PTX), and (c) irinotecan and paclitaxel (Ir + PTX).

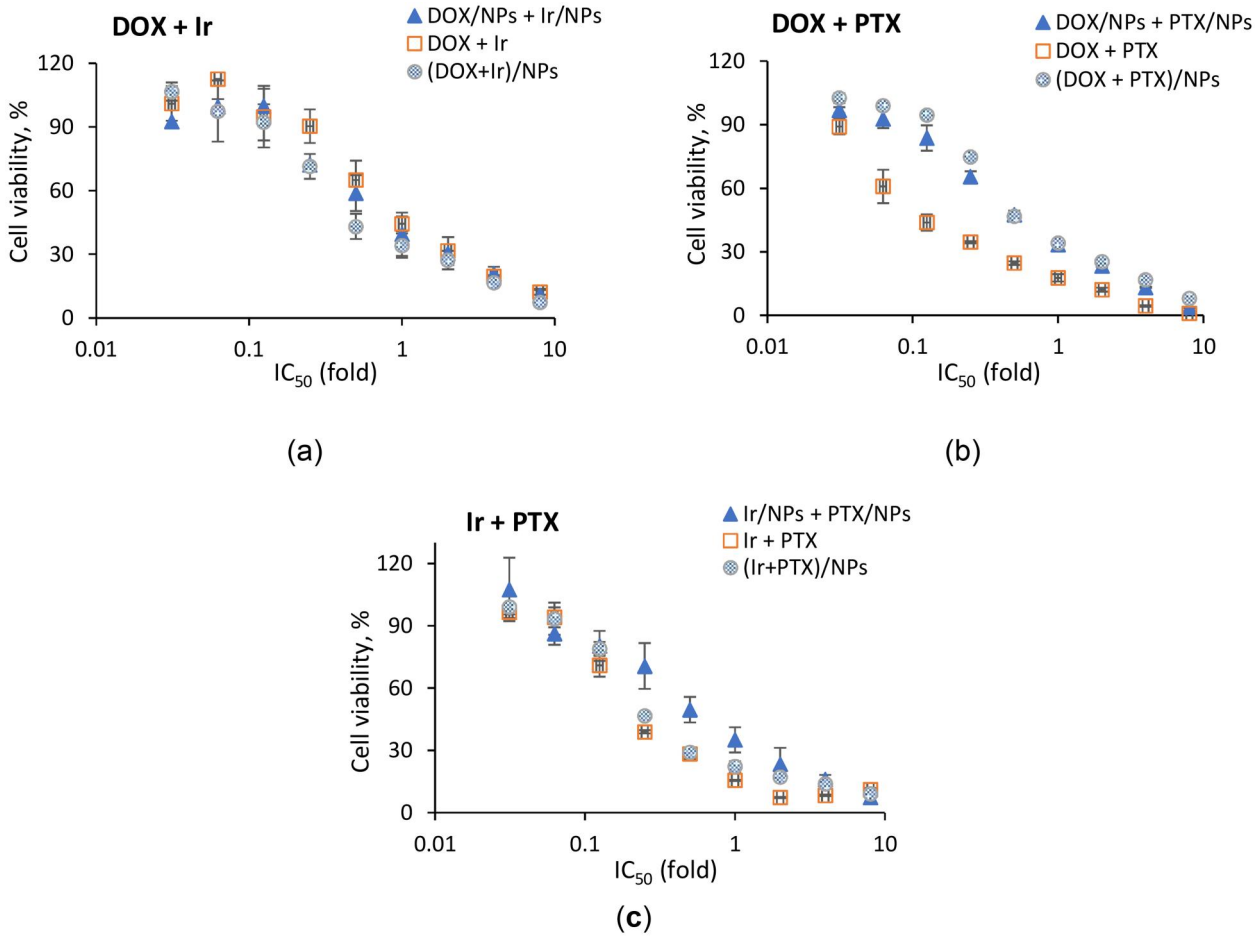

Figure 11. Viability of the colon cancer cells (HCT-116 cell lines) incubated with various forms of combinations of anticancer substances (72 h, $n = 3$): (a) irinotecan and doxorubicin (Ir + DOX), (b) doxorubicin and paclitaxel (DOX + PTX), and (c) irinotecan and paclitaxel (Ir + PTX).

concentrations of substances in the mixture corresponded to IC_{50} or multiples of IC_{50} amounts. In the case of dual-drug encapsulated systems, anti-tumour drugs were encapsulated in one system in such a ratio that their amounts in a particle were equal to the ratio IC_{50} (drug 1)/IC_{50} (drug 2). Viability of cells incubated with different compositions and forms of anti-tumour drugs are presented in Figure 11.

Combinations of doxorubicin with irinotecan (DOX + Ir) and irinotecan with paclitaxel (Ir + PTX) have been shown to work equally well both in (co)encapsulated and free forms. Furthermore, the encapsulation smoothed antagonistic effected of Ir and PTX combination, and the possible reason for this fact is the delayed release of PTX. For the combination of doxorubicin with paclitaxel, the biological activity of (co)encapsulated forms was slightly lower than for a mixture of free substances in the same ratios. However, encapsulated forms significantly increase the solubility of the hydrophobic paclitaxel and may increase its bioavailability.

4. Conclusions

Poly(L-glutamic acid-*co*-D-phenylalanine)-based nanoparticles possessed the required physicochemical characteristics, the absence of cytotoxicity to normal cells and the ability to encapsulate both hydrophobic substances and amphiphilic bases. The size of the (co)encapsulated forms meet the criteria of delivery systems suitable for injections. An advantage of the developed systems is enhanced drug release at weak acidic conditions to provide pH-triggered release in tumours. In addition, the presence of D-Phe-units in the copolymer as well as the negative surface charge and soft nature of the delivery systems will contribute to the delayed blood clearance due to the increased resistance of the polypeptide to enzymatic degradation, opsonisation and uptake by macrophages. The preservation of drug inhibition activity for the encapsulated forms as well as sustained drug release may contribute the improving of drug bioavailability, therapeutic efficacy and overcome multidrug resistance.

Acknowledgements

Centre for Molecular and Cell Technologies of the Research Park of Saint-Petersburg State University is acknowledged for TEM analysis.

Disclosure statement

No potential conflict of interest was reported by the author(s).

Funding

This research was funded by Russian Science Foundation. The work on the development of formulations and some biological experiments was carried out within the project No. 20–73-00222. The release, cytotoxicity and TEM studies were performed as part of project No. 21–73-20104.

References

Ambrosio Téllez, L., *et al.*, 2022. Synthesis and mechanical behavior of poly (vinyl alcohol)/poly (vinyl acetate) microspheres. *Polymer-plastics technology and materials*, 61 (15), 1676–1690. doi: 10.1080/25740881.2022.2075273.

Ambrosio, L., *et al.*, 2023. Anti-tumoral effect of doxorubicin-loaded poly(vinyl alcohol)/poly(vinyl acetate) microspheres in a rat model. *Iranian polymer journal*, 32 (3), 287–297. doi: 10.1007/s13726-022-01121-0.

Batist, G., *et al.*, 2009. Safety, pharmacokinetics, and efficacy of CPX-1 liposome injection in patients with advanced solid tumors. *Clinical cancer research*, 15 (2), 692–700. doi: 10.1158/1078-0432.CCR-08-0515.

D'Angelo, N.A., *et al.*, 2022. Development of PEG-PCL-based polymersomes through design of experiments for co-encapsulation of vemurafenib and doxorubicin as chemotherapeutic drugs. *Journal of molecular liquids*, 349, 118166. doi: 10.1016/j.molliq.2021.118166.

Desale, S.S., *et al.*, 2015. Polypeptide-based nanogels co-encapsulating a synergistic combination of doxorubicin with 17-AAG show potent anti-tumor activity in ErbB2-driven breast cancer models. *Journal of controlled release*, 208, 59–66. doi: 10.1016/j.jconrel.2015.02.001.

Do, H.D., *et al.*, 2018. Folate-modified, curcumin and paclitaxel co-loaded PLA-TPGS nanoparticles: preparation, optimization and in vitro cytotoxicity assays. *Advances in natural sciences*, 9 (2), 025004. doi: 10.1088/2043-6254/aabb5c.

El-Say, K.M., and El-Sawy, H.S., 2017. Polymeric nanoparticles: promising platform for drug delivery. *International journal of pharmaceutics*, 528 (1-2), 675–691. doi: 10.1016/j.ijpharm.2017.06.052.

Ferrari, R., *et al.*, 2018. Polymer nanoparticles for the intravenous delivery of anticancer drugs: the checkpoints on the road from the synthesis to clinical translation. *Nanoscale*, 10 (48), 22701–22719. doi: 10.1039/c8nr05933k.

Gadde, S., 2015. Multi-drug delivery nanocarriers for combination therapy. *MedChemComm*, 6 (11), 1916–1929. doi: 10.1039/C5MD00365B.

Gao, Z., *et al.*, 2020. Polypeptide nanoparticles with pH-sheddable PEGylation for improved drug delivery. *Langmuir*, 36 (45), 13656–13662. doi: 10.1021/acs.langmuir.0c02532.

Georgilis, E., *et al.*, 2020. Nanoparticles based on natural, engineered or synthetic proteins and polypeptides for drug delivery applications. *International journal of pharmaceutics*, 586, 119537. doi: 10.1016/j.ijpharm.2020.119537.

Ghosh, S., *et al.*, 2019. Combinatorial nanocarriers against drug resistance in hematological cancers: Opportunities and emerging strategies. *Journal of controlled release : official journal of the controlled release society*, 296, 114–139. doi: 10.1016/j.jconrel.2019.01.011.

Greco, F., and Vicent, M.J., 2009. Combination therapy: Opportunities and challenges for polymer-drug conjugates as anticancer nanomedicines. *Advanced drug delivery reviews*, 61 (13), 1203–1213. doi: 10.1016/j.addr.2009.05.006.

He, C., *et al.*, 2012. Stimuli-sensitive synthetic polypeptide-based materials for drug and gene delivery. *Advanced healthcare materials*, 1 (1), 48–78. doi: 10.1002/adhm.201100008.

Housman, G., *et al.*, 2014. Drug resistance in cancer: an overview. *Cancers*, 6 (3), 1769–1792. doi: 10.3390/cancers6031769.

Hu, C.M.J., Aryal, S., and Zhang, L., 2010. Nanoparticle-assisted combination therapies for effective cancer treatment. *Therapeutic delivery*, 1 (2), 323–334. doi: 10.4155/tde.10.13.

Hu, Q., *et al.*, 2016. Recent advances of cocktail chemotherapy by combination drug delivery systems. *Advanced drug delivery reviews*, 98, 19–34. doi: 10.1016/j.addr.2015.10.022.

ISO 10993-5. 2009. *Biological evaluation of medical devices—part 5: Tests for in vitro cytotoxicity*.

Iudin, D., *et al.*, 2020. Polypeptide self-assembled nanoparticles as delivery systems for polymyxins B and E. *Pharmaceutics*, 12 (9), 868. doi: 10.3390/pharmaceutics12090868.

Iyer, A.K., *et al.*, 2013. Role of integrated cancer nanomedicine in overcoming drug resistance. *Advanced drug delivery reviews*, 65 (13-14), 1784–1802. doi: 10.1016/j.addr.2013.07.012.

Jacobs, J., *et al.*, 2019. Polypeptide nanoparticles obtained from emulsion polymerization of amino acid N-carboxyanhydrides. *Journal of the American chemical society*, 141 (32), 12522–12526. doi: 10.1021/jacs.9b06750.

Katragadda, U., *et al.*, 2011. Multi-drug delivery to tumor cells via micellar nanocarriers. *International journal of pharmaceutics*, 419 (1-2), 281–286. doi: 10.1016/j.ijpharm.2011.07.033.

Kolishetti, N., *et al.*, 2010. Engineering of self-assembled nanoparticle platform for precisely controlled combination drug therapy. *Proceedings of the national academy of sciences of the united states of america*, 107 (42), 17939–17944. doi: 10.1073/pnas.1011368107.

Levit, M., *et al.*, 2018. Synthesis and characterization of well-defined poly(2-deoxy-2-methacrylamido-d-glucose) and its biopotential block copolymers via RAFT and ROP polymerization. *European polymer journal*. 105, 26–37. doi: 10.1016/j.eurpolymj.2018.05.018.

Levit, M., *et al.*, 2020. Bio-inspired amphiphilic block-copolymers based on synthetic glycopolymer and poly(amino

acid) as potential drug delivery systems. *Polymers*, 12 (1), 183. doi: 10.3390/polym12010183.

Lin, T.L., *et al.*, 2019. A phase 2 study to assess the pharmacokinetics and pharmacodynamics of CPX-351 and its effects on cardiac repolarization in patients with acute leukemias. *Cancer chemotherapy and pharmacology*, 84 (1), 163–173. doi: 10.1007/s00280-019-03856-9.

Lin, X., *et al.*, 2023. Nanoparticles for co-delivery of paclitaxel and curcumin to overcome chemoresistance against breast cancer. *Journal of drug delivery science and technology*, 79, 104050. doi: 10.1016/j.jddst.2022.104050.

Liu, J., *et al.*, 2019. Effective co-encapsulation of doxorubicin and irinotecan for synergistic therapy using liposomes prepared with triethylammonium sucrose octasulfate as drug trapping agent. *International journal of pharmaceutics*, 557, 264–272. doi: 10.1016/j.ijpharm.2018.12.072.

Mansoori, B., *et al.*, 2017. The Different Mechanisms of Cancer Drug Resistance: A Brief Review. *Advanced pharmaceutical bulletin*, 7 (3), 339–348. doi: 10.15171/apb.2017.041.

Marsden, H.R., Gabrielli, L., and Kros, A., 2010. Rapid preparation of polymersomes by a water addition/solvent evaporation method. *Polymer chemistry*, 1 (9), 1512. doi: 10.1039/c0py00172d.

Bruschi, M. L., 2015. Mathematical models of drug release. In *Strategies to modify the drug release from pharmaceutical systems*. Amsterdam: Elsevier, 63–86.

Mehnath, S., *et al.*, 2018. Co-encapsulation of dual drug loaded in MLNPs: Implication on sustained drug release and effectively inducing apoptosis in oral carcinoma cells. *Biomedicine & pharmacotherapy*, 104, 661–671. doi: 10.1016/j.biopha.2018.05.096.

Miao, L., *et al.*, 2017. Nanoformulations for combination or cascade anticancer therapy. *Advanced drug delivery reviews*, 115, 3–22. doi: 10.1016/j.addr.2017.06.003.

Milane, L., Duan, Z., and Amiji, M., 2011. Development of EGFR-targeted polymer blend nanocarriers for combination paclitaxel/lonidamine delivery to treat multi-drug resistance in human breast and ovarian tumor cells. *Molecular pharmaceutics*, 8 (1), 185–203. doi: 10.1021/mp1002653.

Mitchell, M.J., *et al.*, 2021. Engineering precision nanoparticles for drug delivery. *Nature reviews. Drug discovery*, 20 (2), 101–124. doi: 10.1038/s41573-020-0090-8.

Morton, S.W., *et al.*, 2014. A nanoparticle-based combination chemotherapy delivery system for enhanced tumor killing by dynamic rewiring of signaling pathways. *Science signaling*, 7 (325), ra44. doi: 10.1126/scisignal.2005261.

Moughton, A.O., Patterson, J.P., and O'Reilly, R.K., 2011. Reversible morphological switching of nanostructures in solution. *Chemical communications*, 47 (1), 355–357. doi: 10.1039/c0cc02160a.

Patra, J.K., *et al.*, 2018. Nano based drug delivery systems: recent developments and future prospects. *Journal of nanobiotechnology*, 16 (1), 71. doi: 10.1186/s12951-018-0392-8.

Pitchika, S., and Sahoo, S.K., 2022. Paclitaxel and Lapatinib dual loaded chitosan-coated PLGA nanoparticles enhance cytotoxicity by circumventing MDR1-mediated trastuzumab resistance in HER2 positive breast cancers: in-vitro and in-vivo studies. *Journal of drug delivery science and technology*, 73, 103445. doi: 10.1016/j.jddst.2022.103445.

Podgórski, R., Wojasiński, M., and Ciach, T., 2022. Nanofibrous materials affect the reaction of cytotoxicity assays. *Scientific reports*, 12 (1), 9047. doi: 10.1038/s41598-022-13002-w.

Pushpalatha, R., Selvamuthukumar, S., and Kilimozhi, D., 2017. Nanocarrier mediated combination drug delivery for chemotherapy – A review. *Journal of drug delivery science and technology*, 39, 362–371. doi: 10.1016/j.jddst.2017.04.019.

Roell, K.R., Reif, D.M., and Motsinger-Reif, A.A., 2017. An introduction to terminology and methodology of chemical synergy—perspectives from across disciplines. *Frontiers in pharmacology*, 8, 158. doi: 10.3389/fphar.2017.00158.

Roque, M.C., *et al.*, 2021. Preclinical toxicological study of long-circulating and fusogenic liposomes co-encapsulating paclitaxel and doxorubicin in synergic ratio. *Biomedicine & pharmacotherapy*, 144, 112307. doi: 10.1016/j.biopha.2021.112307.

Shah, M., *et al.*, 2012. Biodegradation of elastin-like polypeptide nanoparticles. *Protein science : a publication of the protein society*, 21 (6), 743–750. doi: 10.1002/pro.2063.

Tardi, P., *et al.*, 2009. In vivo maintenance of synergistic cytarabine:daunorubicin ratios greatly enhances therapeutic efficacy. *Leukemia research*, 33 (1), 129–139. doi: 10.1016/j.leukres.2008.06.028.

Tardi, P.G., *et al.*, 2007. Coencapsulation of irinotecan and floxuridine into low cholesterol-containing liposomes that coordinate drug release in vivo. *Biochimica et biophysica acta*, 1768 (3), 678–687. doi: 10.1016/j.bbamem.2006.11.014.

Tardi, P.G., *et al.*, 2009. Drug ratio-dependent antitumor activity of irinotecan and cisplatin combinations in vitro and in vivo. *Molecular cancer therapeutics*, 8 (8), 2266–2275. doi: 10.1158/1535-7163.MCT-09-0243.

Tian, J., *et al.*, 2017. Nanoparticle delivery of chemotherapy combination regimen improves the therapeutic efficacy in mouse models of lung cancer. *Nanomedicine : nanotechnology, biology, and medicine*, 13 (3), 1301–1307. doi: 10.1016/j.nano.2016.11.007.

Vichai, V., and Kirtikara, K., 2006. Sulforhodamine B colorimetric assay for cytotoxicity screening. *Nature protocols*, 1 (3), 1112–1116. doi: 10.1038/nprot.2006.179.

Wang, X., *et al.*, 2021. Polypeptide-based drug delivery systems for programmed release. *Biomaterials*, 275, 120913. doi: 10.1016/j.biomaterials.2021.120913.

Williams, J., *et al.*, 2003. Nanoparticle drug delivery system for intravenous delivery of topoisomerase inhibitors. *Journal of controlled release*, 91 (1-2), 167–172. doi: 10.1016/s0168-3659(03)00241-4.

Xiao, B., *et al.*, 2015a. Co-delivery of camptothecin and curcumin by cationic polymeric nanoparticles for synergistic colon cancer combination chemotherapy. *Journal of materials chemistry B*, 3 (39), 7724–7733. doi: 10.1039/c5tb01245g.

Xiao, B., *et al.*, 2015b. Hyaluronic acid-functionalized polymeric nanoparticles for colon cancer-targeted combination chemotherapy. *Nanoscale*, 7 (42), 17745–17755. doi: 10.1039/c5nr04831a.

Xu, L., *et al.*, 2022. Lipid Nanoparticles for Drug Delivery. *Adv. NanoBiomed res*, 2, 2100109.

Xu, X., *et al.*, 2015. Cancer nanomedicine: From targeted delivery to combination therapy. *Trends in molecular medicine*, 21 (4), 223–232. doi: 10.1016/j.molmed.2015.01.001.

Yang, Q., *et al.*, 2014. Coencapsulation of epirubicin and metformin in PEGylated liposomes inhibits the recurrence of murine sarcoma S180 existing CD133+ cancer stem-like cells. *European journal of pharmaceutics and biopharmaceutics* 88 (3), 737–745. doi: 10.1016/j.ejpb.2014.10.006.

Yang, S., *et al.*, 2022. Drug-free neutrally charged polypeptide nanoparticles as anticancer agents. *Journal of controlled release*, 345, 464–474. doi: 10.1016/j.jconrel.2022.03.034.

Yao, Y., *et al.*, 2020. Nanoparticle-based drug delivery in cancer therapy and its role in overcoming drug resistance. *Frontiers in molecular biosciences*, 7, 193. doi: 10.3389/fmolb.2020.00193.

Zashikhina, N., *et al.*, 2019. Novel formulations of C-peptide with long-acting therapeutic potential for treatment of diabetic complications. *Pharmaceutics*, 11 (1), 27. doi: 10.3390/pharmaceutics11010027.

Zashikhina, N., *et al.*, 2021. Synthesis and characterization of macroinitiators based on polyorganophosphazenes for the ring opening polymerization of n-carboxyanhydrides. *Polymers*, 13 (9), 1446. doi: 10.3390/polym13091446.

Zashikhina, N., *et al.*, 2022. Biocompatible nanoparticles based on amphiphilic random polypeptides and glycopolymers as drug delivery systems. *Polymers*, 14 (9), 1677. doi: 10.3390/polym14091677.

Zashikhina, N.N., *et al.*, 2017. Self-assembled polypeptide nanoparticles for intracellular irinotecan delivery. *European journal of pharmaceutical sciences*, 109, 1–12. doi: 10.1016/j.ejps.2017.07.022.

Zhang, X., *et al.*, 2016. EGF-modified mPEG-PLGA-PLL nanoparticle for delivering doxorubicin combined with Bcl-2 siRNA as a potential treatment strategy for lung cancer. *Drug delivery*, 23 (8), 2936–2945. doi: 10.3109/10717544.2015.1126769.

Zhang, Y., *et al.*, 2010. DDSolver: an add-in program for modeling and comparison of drug dissolution profiles. *The AAPS journal*, 12 (3), 263–271. doi: 10.1208/s12248-010-9185-1.

Zhang, Y., *et al.*, 2016. Co-delivery of doxorubicin and curcumin by pH-sensitive prodrug nanoparticle for combination therapy of cancer. *Scientific reports*, 6, 21225. doi: 10.1038/srep21225.

Zheng, C., *et al.*, 2013. Polypeptide cationic micelles mediated co-delivery of docetaxel and siRNA for synergistic tumor therapy. *Biomaterials*, 34 (13), 3431–3438. doi: 10.1016/j.biomaterials.2013.01.053.

Zhou, J., *et al.*, 2020. The drug-resistance mechanisms of five platinum-based antitumor agents. *Frontiers in pharmacology*, 11, 343. doi: 10.3389/fphar.2020.00343.